DEUTSCHES ELEKTRONEN-SYNCHROTRON DESY

DESY 67/30
October 1967

PHOTOPRODUCTION OF ρ^0 MESONS ON HYDROGEN, CARBON AND ALUMINIUM WITH PHOTONS OF KNOWN ENERGY

by

H. Blechschmidt, J.P. Dowd, B. Elsner, K. Heinloth, K.H. Höhne, S. Raither, J. Rathje, D. Schmidt, J.H. Smith, J.H. Weber

Deutsches Elektronen-Synchrotron DESY, Hamburg, Germany

2 HAMBURG 52 · NOTKESTIEG 1

PHOTOPRODUCTION OF ρ^0 MESONS ON HYDROGEN, CARBON AND ALUMINIUM WITH PHOTONS OF KNOWN ENERGY

by

H. Blechschmidt, J.P. Dowd[+], B. Elsner, K. Heinloth, K.H. Höhne, S. Raither, J. Rathje, D. Schmidt, J.H. Smith[++], J.H. Weber

Deutsches Elektronen-Synchrotron DESY, Hamburg, Germany

[+] Present address: SMTI, New Bedford, Massachusetts, U.S.A.

[++] Present address: University of Illinois, Urbana, Illinois, U.S.A.;

supported by Volkswagen Foundation.

In a spark-chamber experiment photoproduction of pion pairs on hydrogen, carbon and aluminium has been investigated at photon energies between 3.2 and 4.9 GeV. For each event the photon energy was measured with an accuracy of ±50 MeV.

(1) $$\gamma + A \rightarrow A + \pi^+ + \pi^-$$

The main object of our investigation was the production of ρ^o mesons.

(2) $$\gamma + A \rightarrow A + \rho^o$$

1. Experimental Setup

The experimental setup is shown in Fig. 1. A bremsstrahlung beam of $2 \cdot 10^5$ effective quanta/sec is produced by conversion of a positron beam in the tantalum target TA. The energy of the photon is determined by measuring the momenta of the associated positrons[1]. This is done using a horizontally focusing bending magnet MD and an array of 29 scintillation counters (tagging system).

The positron beam intensity is monitored by the ionization chamber I.CH., which was calibrated against a quantameter during the experiment. The photon beam is absorbed inside the magnet MH by the tungsten block A.

In the detection apparatus[2] consisting of two pairs of spark-chambers and the deflection magnet MH, production angles and momenta of the produced charged particles are measured. Pions are identified by a threshold Čerenkov counter Č and two thick-plate spark-chambers SC5 and SC6. Pictures were taken whenever two charged particles passed the spark-chamber system. Out of the 13,000 pictures taken we got 1,500 events for our analysis.

The acceptance Acc of our apparatus for detecting a two particle system was calculated as a threefold integral over the azimuthal angle and the polar angle θ_N^* of the positive particle in the two-particle rest system with respect to the direction of the recoiling target particle and the azimuthal angle of the combined system. For the polar angle θ_N^* a $\sin^2$ distribution was assumed due to previous measurements on the ρ^o [3].

2. Results

To separate the process (1) from reactions where additional particles were produced, we consider the difference Δk between the measured photon energy k and the photon energy computed from the measured momenta of the two pions under the assumption that the process (1) has occurred. From the Δk distribution shown in Fig. 2 we deduce that all the events which lie in the range $-0.2\ \text{GeV} < \Delta k < +0.2\ \text{GeV}$ are due to the reaction (1). No evidence is seen for production of ρ^o mesons together with a nucleon resonance. The invariant mass spectrum of the two pion system produced on H_2, C and Al is shown in Fig. 3. The mass distributions were fitted to a Breit-Wigner function plus a phenomenological background function expressed in terms of powers of $m_{\pi\pi}$. The Breit-Wigner function was multiplied with an additional factor $m_\rho{}^4/m_{\pi\pi}{}^4$ stemming from a photon dissociation model[9]. The best fit values are:

$m_\rho = 764 \pm 12$ MeV, $\Gamma_\rho = 124 \pm 15$ MeV, fraction 98 % ρ^o for H_2;

$m_\rho = 777 \pm 12$ MeV, $\Gamma_\rho = 126 \pm 15$ MeV, fraction 98 % ρ^o for C;

$m_\rho = 770 \pm 12$ MeV, $\Gamma_\rho = 117 \pm 15$ MeV, fraction 97 % ρ^o for Al.

Without the mass-skewing factor $m_\rho{}^4/m_{\pi\pi}{}^4$ we obtain values for ρ^o masses which lie about 20 MeV lower. The given mass values are in good agreement with other experiments[4,5,6,7,8].

The differential cross section $\frac{d\sigma}{dt}$ as a function of the square of the four-momentum transfer to the recoil nucleon t is shown for the different targets in Fig. 4. Since our data show the typical diffraction behaviour[10,11], we fitted them with:

$$\frac{d\sigma}{dt} = a \cdot e^{bt} \quad \frac{\text{mb}}{\text{GeV}^2 \text{ nucleus}}$$

This gives the following values:

$a = 0.125 \pm 0.015 \frac{mb}{GeV^2}$, $b = 8.1 \pm 1.5\ GeV^{-2}$ for H_2;

$a = 8.2 \pm 1.0 \frac{mb}{GeV^2\ nucleus}$; $b = 47.8 \pm 4.6\ GeV^{-2}$ for C;

$a = 31.7 \pm 5 \frac{mb}{GeV^2\ nucleus}$, $b = 73.0 \pm 9.3\ GeV^{-2}$ for Al.

We find the coefficient b proportional to $A^{2/3}$ where A is the mass number of the target nuclei. a is found to be proportional to $A^{1.68 \pm 0.1}$. This shows a behaviour of the nucleus between opacity and transparency.

The total cross section for the process $\gamma + A \rightarrow \rho^o + A$ was determined by extrapolation of the differential cross section $\frac{d\sigma}{dt}$ to high $|t|$ values and integration over t. We get the values

$\sigma_{tot} = 14.6 \pm 1.8\ \mu b$ for H_2 and $3.2 < k < 4.9$ GeV,

$\sigma_{tot} = 130 \pm 22 \frac{\mu b}{nucleus}$ for C and $3.2 < k < 4.4$ GeV,

$\sigma_{tot} = 284 \pm 40 \frac{\mu b}{nucleus}$ for Al and $3.2 < k < 4.4$ GeV.

The angular distribution $\frac{d\sigma}{d\Omega^*}$ of the ρ^o mesons in the center of mass system for the different targets is shown in Fig. 5.

In Fig. 6 the energy dependence of the forward cross section $\frac{d\sigma}{d\Omega}$ in the lab system is given. It shows a k^2 behaviour in accordance with diffraction production.

We checked also the angular distribution of the decay pions in the ρ^o rest system with respect to the incoming photon (Gottfried-Jackson angle) and to the outgoing nucleon (helicity angle) and found good agreement with bubble chamber results[4,5] within our accepted range.

Acknowledgements

We wish to thank Professors W. Jentschke and P. Stähelin for their continued interest and encouragement in this experiment. We are very much indebted to the DESY Rechenzentrum, the Hallendienst and the synchrotron staff for their excellent cooperation and support. We thank Dr. A. Kanaris and Mr. T. Wynroe for their help during the experiment. We also thank Dr. A. Ladage for the calibration measurement of the beam, Dr. G. Schultze and Mr. F. Selonke for the construction and the test of the Cerenkov Counter and Miss H. Freier, Mr. J. Palm, Mr. R. Globisch and our scanning girls for their continuous help.

Literature

(1) This principle was earlier described by Caldwell et al., Rev. Sc. Instr. 36, 283 (1965).

(2) This detection apparatus was also used in an experiment of pion electroproduction by H. Blechschmidt et al., (to be published).

(3) J.D. Jackson, Nuov. Cim. 34, 1644 (1964).

(4) DESY Bubble Chamber Collaboration, Nuov. Cim. 41, 270 (1966).

(5) CEA Bubble Chamber, Phys. Rev. 146, 994 (1966)

(6) L.J. Lanzerotti et al., Phys. Rev. Lett. 15, 210 (1965).

(7) H. Blechschmidt et al., Proc. Int. Symp. on Electron and Photon Interactions, p. 173, Hamburg 1965.

(8) J.G. Asbury et al., Phys. Rev. Letters 19, 865 (1967).

(9) M. Ross and L. Stodolsky, Phys. Rev. 149, 1172 (1966).

(10) S.D. Drell and J.S. Trefil, Phys. Rev. Lett. 16, 552 (1966).

(11) S.M. Berman and S.D. Drell, Phys. Rev. 133, B 791 (1964).

Figure Captions

Fig. 1 Experimental setup.

Fig. 2 Distribution of the difference Δk between measured photon energy and photon energy calculated under the assumption that the reaction $\gamma + A \rightarrow A + \pi^+ + \pi^-$ has occurred.

Fig. 3 $(\pi^+\pi^-)$ mass spectrum for H_2, C and Al target. Solid curves show fits of Breit-Wigner distributions multiplied with $(m_\rho{}^4/m_{\pi\pi}{}^4)$.

Fig. 4 Differential cross section $\frac{d\sigma}{dt}$ as a function of the four momentum transfer square t for H_2, C and Al target.

Fig. 5 Distribution of the ρ^o meson production angles in the center of mass system.

Fig. 6 Energy dependence of the differential cross section $\frac{d\sigma}{d\Omega}$ in forward direction. For comparison a k^2 dependence is drawn into the figures (dash-dotted curves).

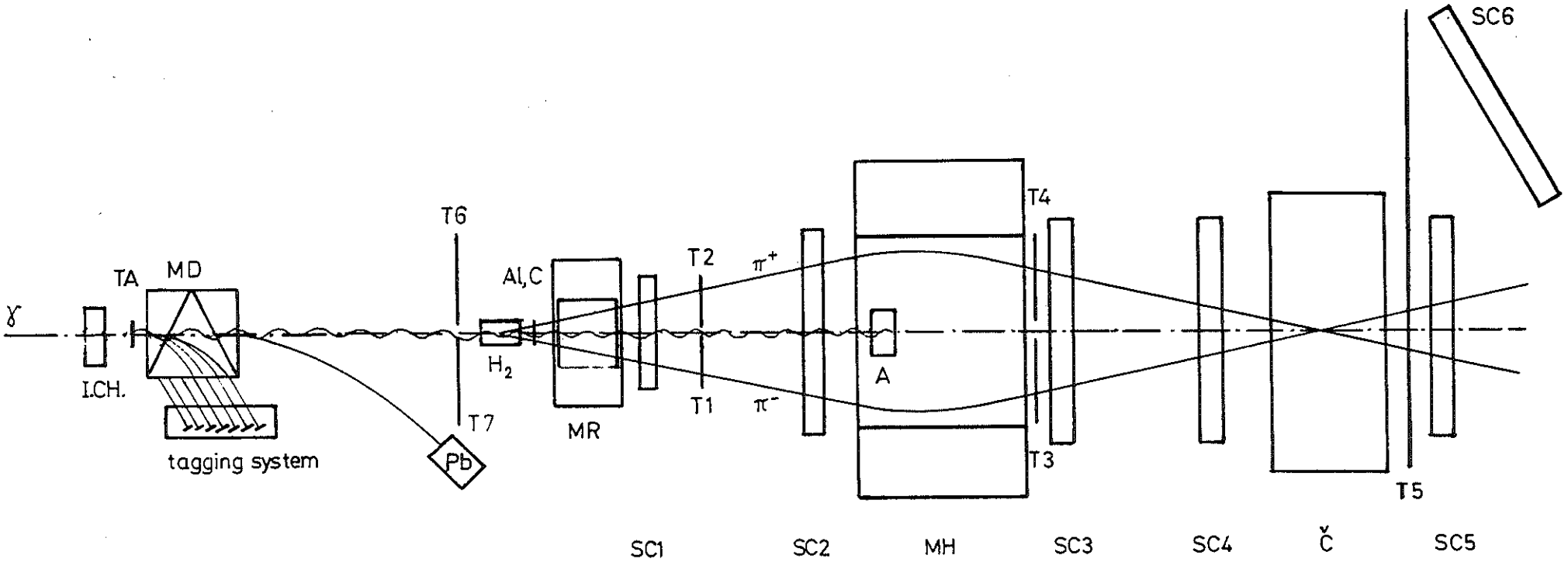
γ
I.CH.
TA
MD
tagging system
T6
T7
Pb
H_2
Al,C
MR
T2
T1
π^+
π^-
SC1
SC2
A
MH
T4
T3
SC3
SC4
Č
T5
SC5
SC6

Fig.1

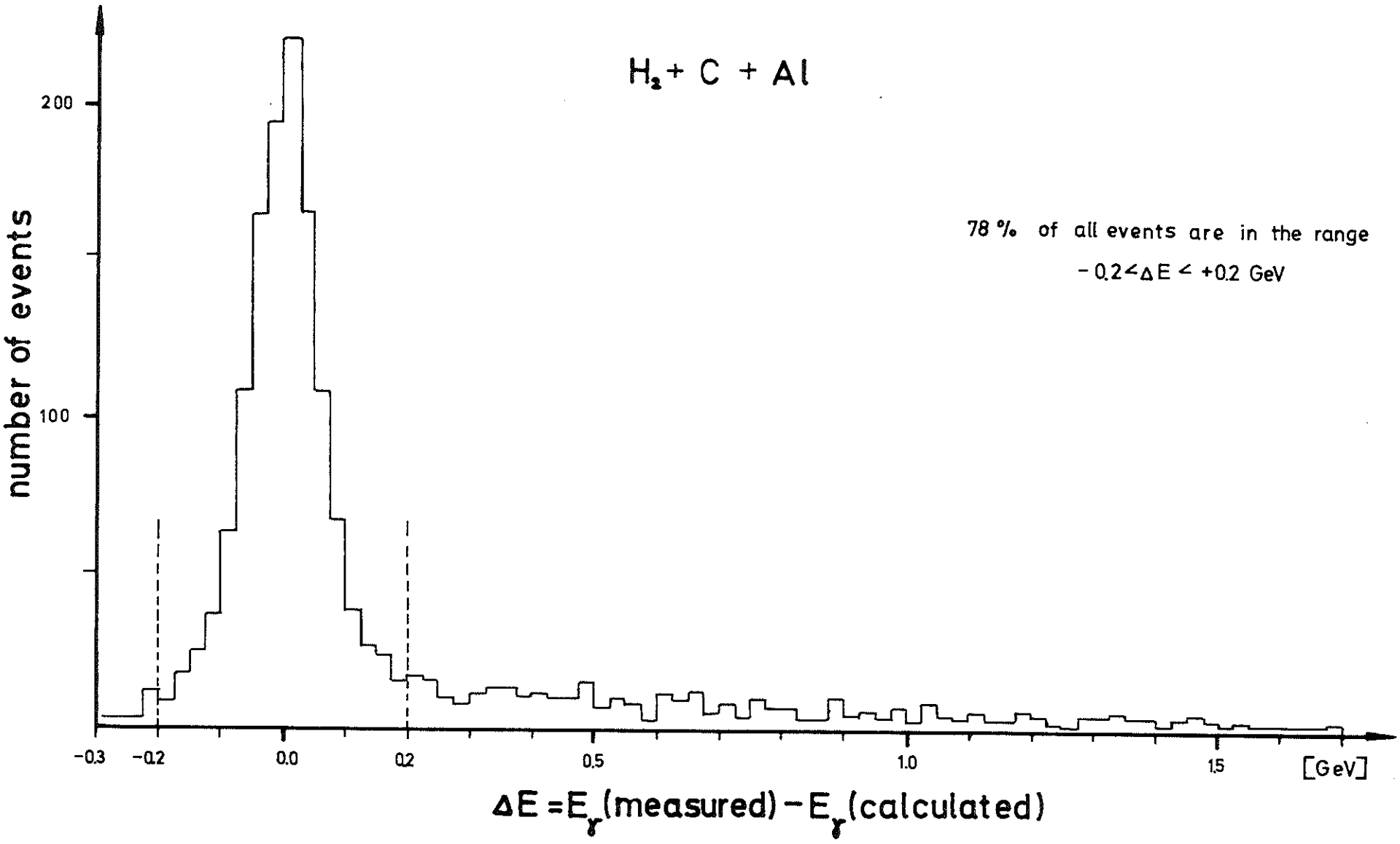
H_2 + C + Al
78 % of all events are in the range
$-0.2 < \Delta E < +0.2$ GeV
number of events
200
100
-0.3
-0.2
0.0
0.2
0.5
1.0
1.5
[GeV]
$\Delta E = E_\gamma$(measured) $- E_\gamma$(calculated)

Fig.2

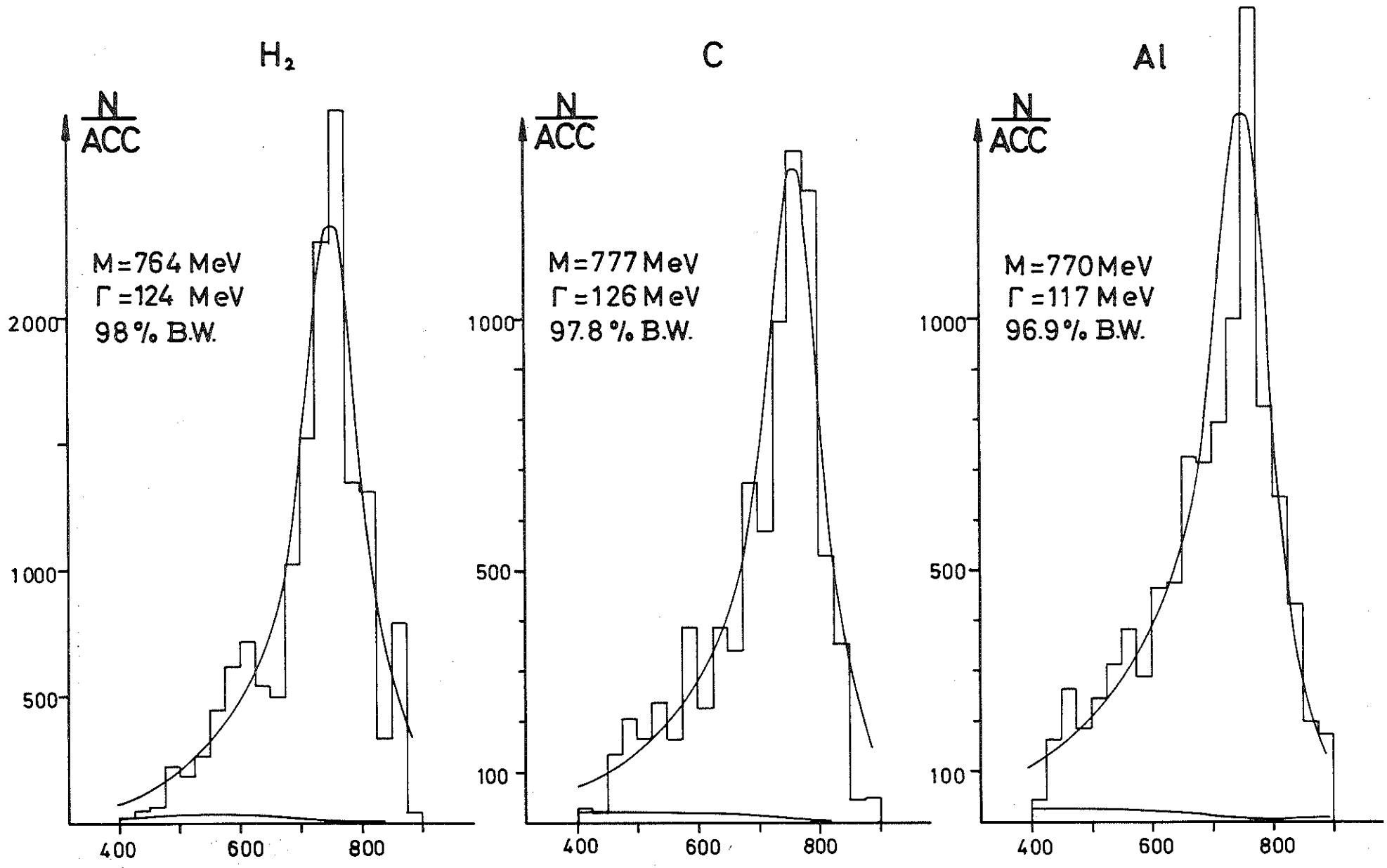
H₂
C
Al
N/ACC
M=764 MeV
Γ=124 MeV
98 % B.W.
M=777 MeV
Γ=126 MeV
97.8 % B.W.
M=770 MeV
Γ=117 MeV
96.9 % B.W.
2000
1000
500
1000
500
100
1000
500
100
400
600
800
M(π⁺π⁻)[MeV]

Fig. 3

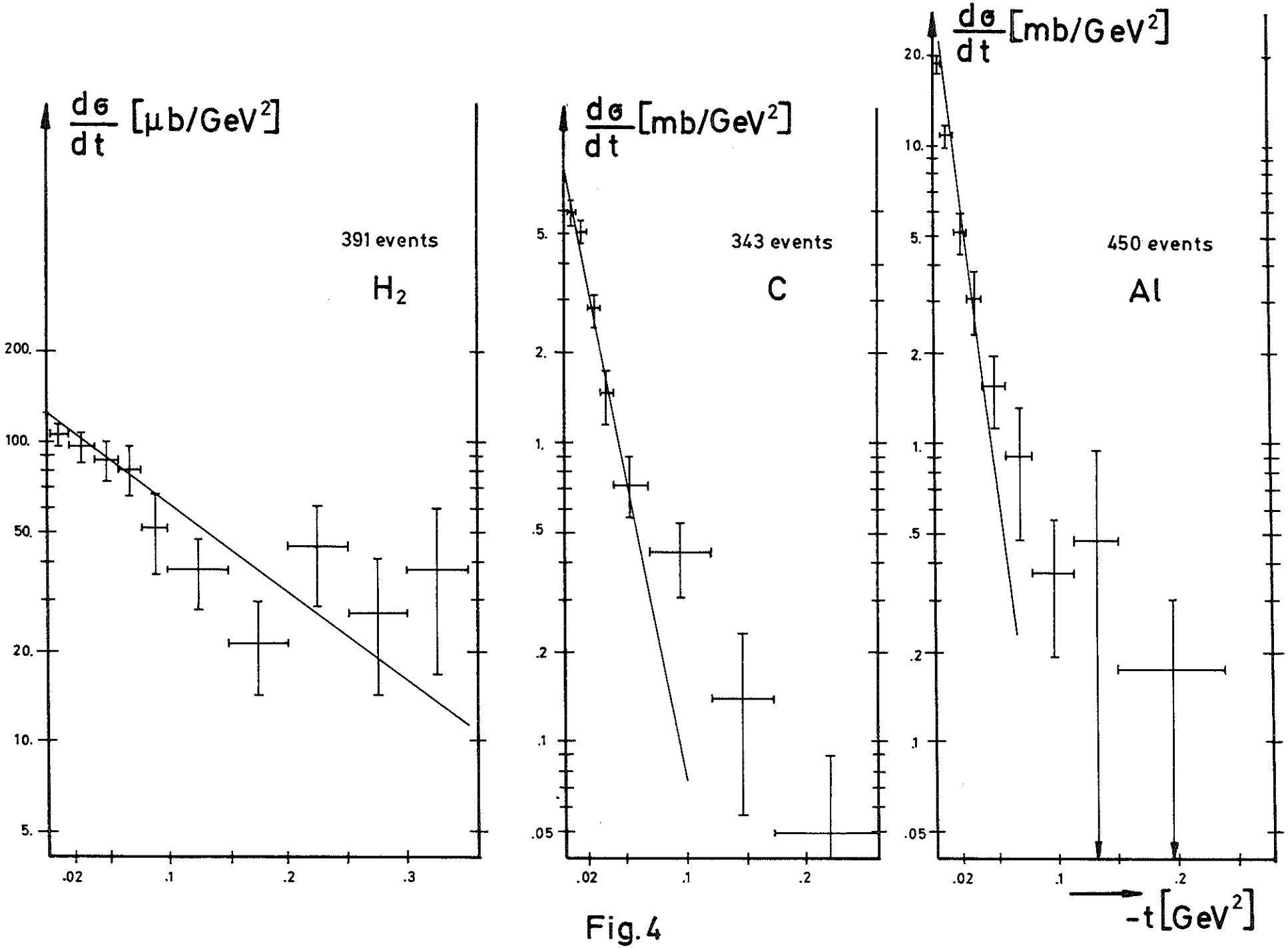
dσ/dt [μb/GeV²]
391 events
H2
200.
100.
50.
20.
10.
5.
.02
.1
.2
.3
dσ/dt [mb/GeV²]
343 events
C
5.
2.
1.
.5
.2
.1
.05
.02
.1
.2
dσ/dt [mb/GeV²]
450 events
Al
20.
10.
5.
2.
1.
.5
.2
.1
.05
.02
.1
.2
-t [GeV²]

Fig. 4

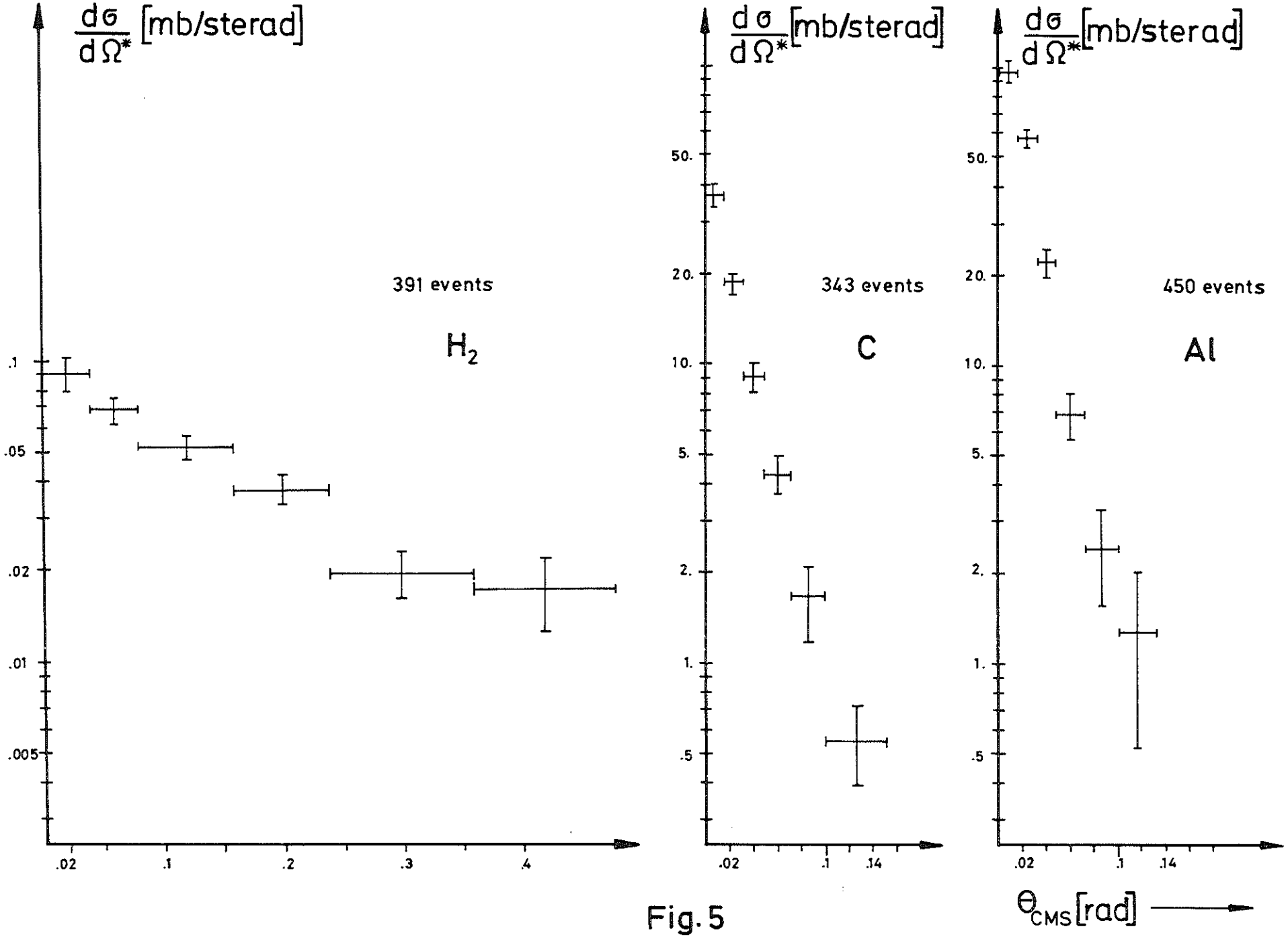
dσ/dΩ* [mb/sterad]
391 events
H2
343 events
C
450 events
Al
.1
.05
.02
.01
.005
50.
20.
10.
5.
2.
1.
.5
.02
.1
.2
.3
.4
.14
θCMS [rad]

Fig. 5

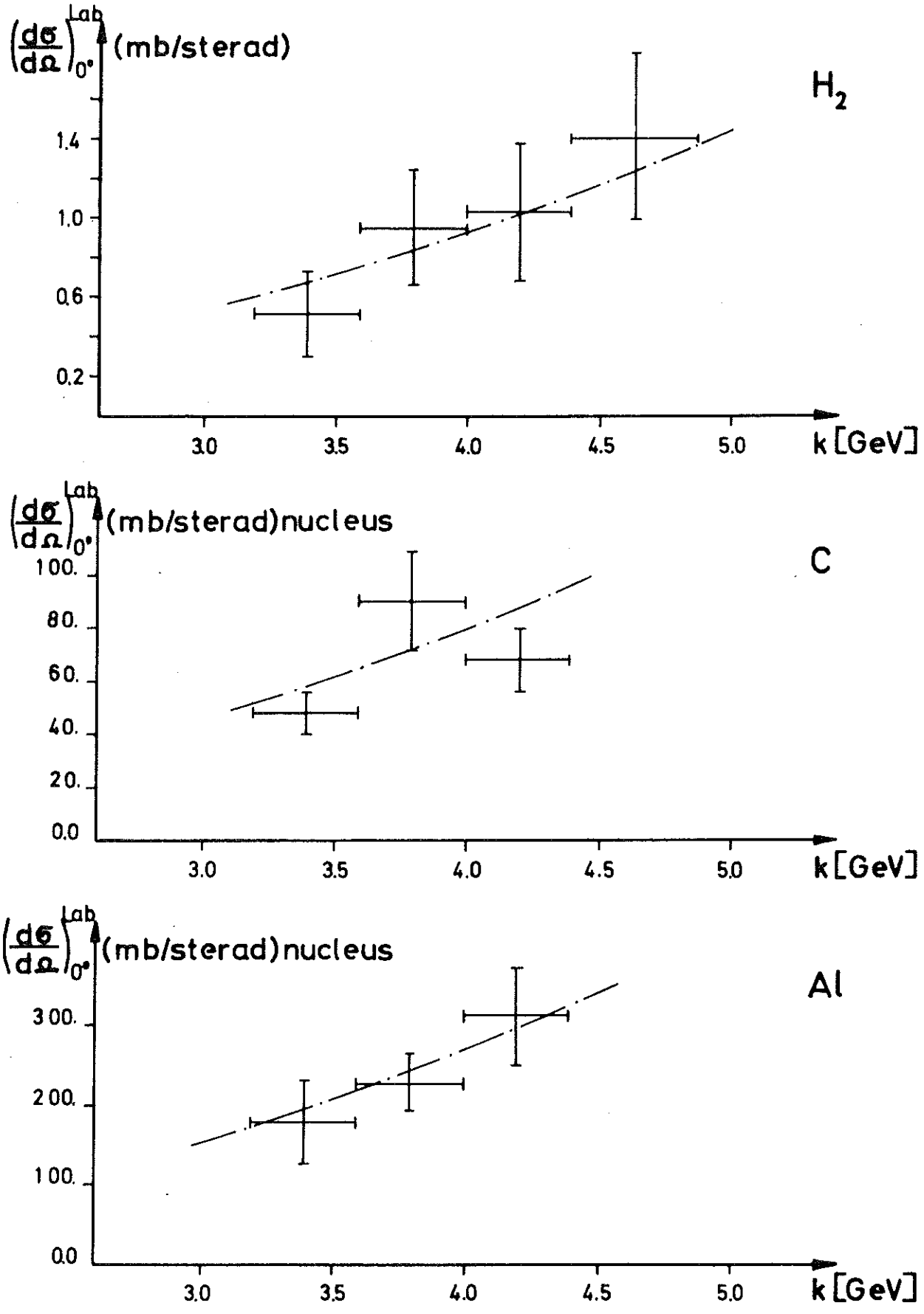
$\left(\frac{d\sigma}{d\Omega}\right)^{Lab}_{0^\circ}$ (mb/sterad)
H_2
1.4
1.0
0.6
0.2
3.0
3.5
4.0
4.5
5.0
k [GeV]
$\left(\frac{d\sigma}{d\Omega}\right)^{Lab}_{0^\circ}$ (mb/sterad) nucleus
C
100.
80.
60.
40.
20.
0.0
3.0
3.5
4.0
4.5
5.0
k [GeV]
$\left(\frac{d\sigma}{d\Omega}\right)^{Lab}_{0^\circ}$ (mb/sterad) nucleus
Al
300.
200.
100.
0.0
3.0
3.5
4.0
4.5
5.0
k [GeV]

Fig.6